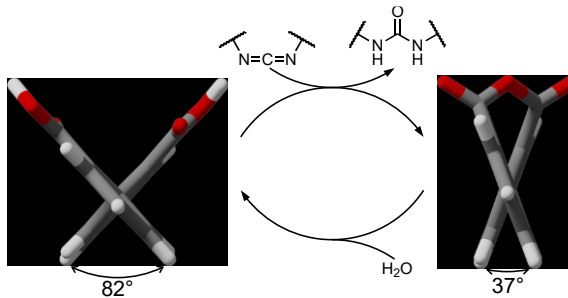


# Chemically Fueled Transient Geometry Changes in Diphenic Acids

Isuru M. Jayalath, Hehe Wang, Georgia Mantel, Lasith S. Kariyawasam, and C. Scott Hartley\*

Department of Chemistry & Biochemistry, Miami University, Oxford, Ohio 45056, United States

Supporting Information Placeholder



**ABSTRACT:** Transient changes in molecular geometry are key to the function of many important biochemical systems. Here, we show that diphenic acids undergo out-of-equilibrium changes in dihedral angle when reacted with a carbodiimide chemical fuel. Treatment of appropriately functionalized diphenic acids with EDC (*N*-(3-dimethylaminopropyl)-*N'*-ethylcarbodiimide hydrochloride) yields the corresponding diphenic anhydrides, reducing the torsional angle about the biaryl bond by approximately 45°, regardless of substitution. In the absence of steric resistance, the reaction is well-described by a simple mechanism; the resulting kinetic parameters can be used to derive important properties of the system, such as yields and lifetimes. The reaction tolerates steric hindrance ortho to the biaryl bond, although the competing formation of (transient) byproducts complicates quantitative analysis.

Many biochemical systems operate in out-of-equilibrium states that require a continuous supply of energy to maintain function.<sup>1,2</sup> This “dissipative” behavior<sup>3,4</sup> imparts properties, such as temporal control, that cannot be achieved at thermodynamic equilibrium.<sup>5</sup> Out-of-equilibrium geometry changes play a vital role in this context.<sup>6–8</sup> For example, geometry changes are fundamental to the operation of ATP-fueled molecular motor proteins;<sup>6,7</sup> these changes are associated with multiple cell functions, including intracellular trafficking,<sup>6</sup> active transport,<sup>8</sup> cell division,<sup>9</sup> signal transduction,<sup>10</sup> and protein translocation.<sup>10</sup>

Inspired by nature’s example, nonbiological out-of-equilibrium behavior driven by chemical fuels has recently attracted considerable attention.<sup>11–13</sup> Recent work from Boekhoven,<sup>14,15</sup> our group,<sup>16,17</sup> Das,<sup>18,19</sup> and others<sup>20,21</sup> has shown that carbodiimides, typically EDC (*N*-(3-dimethylaminopropyl)-*N'*-ethylcarbodiimide hydrochloride), are useful fuels for abiotic nonequilibrium behavior. In a typical system, aqueous carboxylic acids react with carbodiimides to form carboxylic anhydrides, which subsequently undergo hydrolysis to regenerate the original carboxylic acids.

Unlike other chemical fuels (e.g., alkylating agents<sup>11</sup>), carbodiimides form a transient bond between two independent components. Consequently, they can be used to form intramolecular bonds,<sup>22</sup> a potentially useful tool for inducing changes in geometry. Here, we demonstrate a simple system that undergoes significant changes in the twist about a

single bond on treatment with a chemical fuel.<sup>23</sup> Our focus is the water-soluble diphenic acids shown in Figure 1a. Anhydride bond formation was expected to lead to a substantial decrease in the dihedral angle about the biaryl axis. The system acts as a sort of molecular clamp, distinct from other systems that undergo non-equilibrium conformational switching.<sup>24</sup> Of course, this unaggregated, single-molecule system is much simpler than the ATP-fueled biological systems that serve as its inspiration, but the fundamental concept is similar.

Diphenic acid derivatives **DP-Ac1–DP-Ac3** were designed to include hexaglyme groups for water solubility and a small selection of R groups to test the ability of the chemistry to work against steric resistance. DFT geometry optimizations (B97-D3(BJ)/TZV(2d,2p), gas phase, Figure 1b) show that the dihedral angle about the biaryl bond in diphenic acid ( $\phi_{\text{acid}}$ ) is nearly orthogonal, as shown in Table 1. Bridging via anhydride formation reduces the twist ( $\phi_{\text{anhydride}}$ ), with a net change  $\Delta\phi$  of 45°. Ethynyl and ethyl substituents ortho to the biaryl bond increase both  $\phi_{\text{acid}}$  and  $\phi_{\text{anhydride}}$ , but the net change is predicted to be similar in all three cases.

The syntheses of the target compounds began with commercially available diphenic acid **1**, as shown in Scheme 1. The synthesis of **DP-Ac1** was straightforward from compound **4** (Scheme 1a), which was synthesized following a known procedure.<sup>25</sup> The key intermediate for the syntheses

of **DP-Ac2** and **DP-Ac3**, dimethyl 6-bromo-4,4'-dinitro-2,2'-biphenyldicarboxylate **6**, was obtained from the monobromination of known<sup>25</sup> compound **2** using NBS (Scheme 1b). It was reduced, diazotized, and hydrolyzed to form intermediate **8**. Sonogashira coupling with TMS-acetylene introduced the acetyl group in **9**. This intermediate was converted to **DP-Ac2** by alkylation, giving **10** (deprotection of the TMS group occurs simultaneously), followed by saponification. This same intermediate (**10**) was subjected to catalytic hydrogenation and saponification to give **DP-Ac3**.

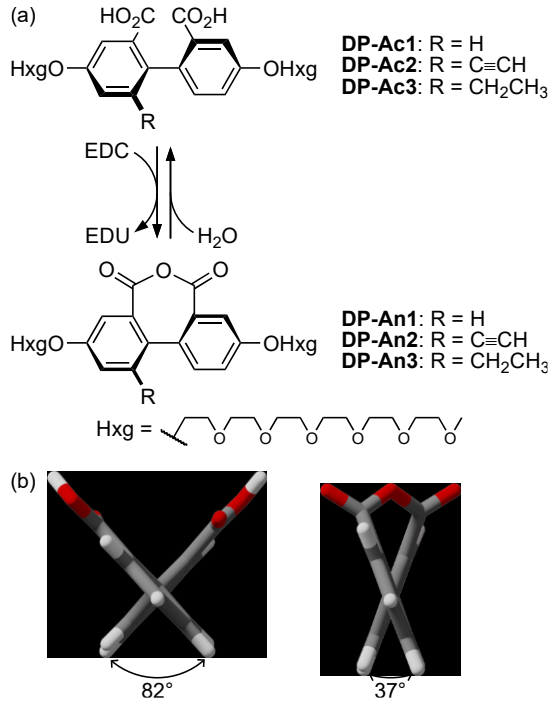
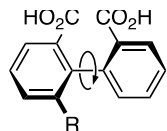


**Figure 1.** (a) Transient anhydride formation in the diphenic acids used in this work. (b) Model acid and anhydride geometries (R = H, OHxg removed) optimized at the B97-D3(BJ)/TZV(2d,2p) level and viewed down the biaryl axis.

**Table 1.** Biaryl dihedral angles of diphenic acids and their anhydrides calculated at the B97-D3(BJ)/TZV(2d,2p) level.

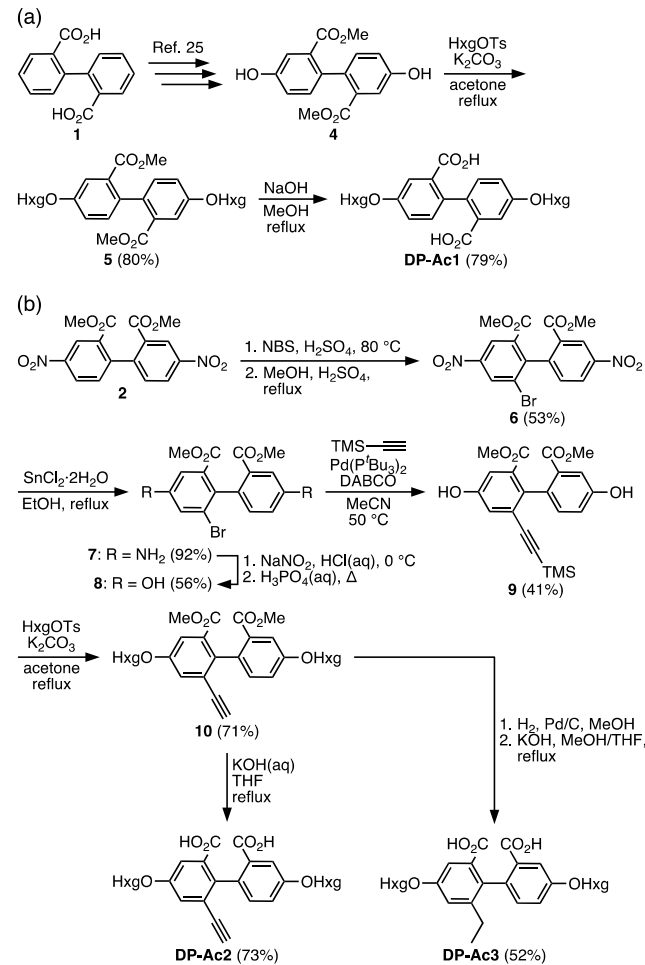


R	$\phi_{\text{acid}}$	$\phi_{\text{anhydride}}$	$\Delta\phi$
H	82°	37°	45°
CCH	91°	44°	47°
CH <sub>2</sub> CH <sub>3</sub>	91°	50°	41°

The formation of anhydride **DP-An1** from **DP-Ac1** was first monitored by in situ IR spectroscopy. Treatment of an aqueous solution of **DP-Ac1** with 0.5 equiv of EDC resulted in the appearance of two peaks at 1775 cm<sup>-1</sup> and 1738 cm<sup>-1</sup> (Figure S1) which are characteristic of the symmetric and asymmetric carbonyl stretching modes of diphenic anhydrides.<sup>26</sup> These experiments were carried out at relatively low temperature (278 K) to slow down the rate of anhydride hydrolysis. Monitoring of the reaction in D<sub>2</sub>O by <sup>1</sup>H

NMR spectroscopy was also consistent with the effective formation of the anhydride (Figures S6–S8). To further confirm that the transient species is indeed the anhydride, an authentic sample of **DP-An1** was synthesized, fully characterized, and compared with the experimental results (see Supporting Information). It is evident that formation of the intramolecular anhydride is dominant under these conditions, presumably because cyclization is favored at these relatively low concentrations and steric hindrance disfavors intermolecular coupling.

**Scheme 1. Syntheses of diphenic acids (a) DP-Ac1 and (b) DP-Ac2/DP-Ac3.**



We later found water:acetone mixtures to be better solvents for **DP-Ac2** and **DP-Ac3** (see below). Accordingly, the remaining experiments for **DP-Ac1** were carried out in 7:3 D<sub>2</sub>O:acetone-*d*<sub>6</sub> at 276 K. A typical reaction of 25 mM **DP-Ac1** with 40 mM EDC at 276 K as monitored by <sup>1</sup>H NMR spectroscopy is shown in Figure 2a. The **DP-Ac1** is rapidly consumed with the associated appearance of signals assigned to **DP-An1**. The EDC was concomitantly converted to EDU (not shown). The anhydride **DP-An1** cleanly hydrolyzes back to its parent acid **DP-Ac1** over the course of minutes. The full time course of the experiment is shown in Figure 2b.

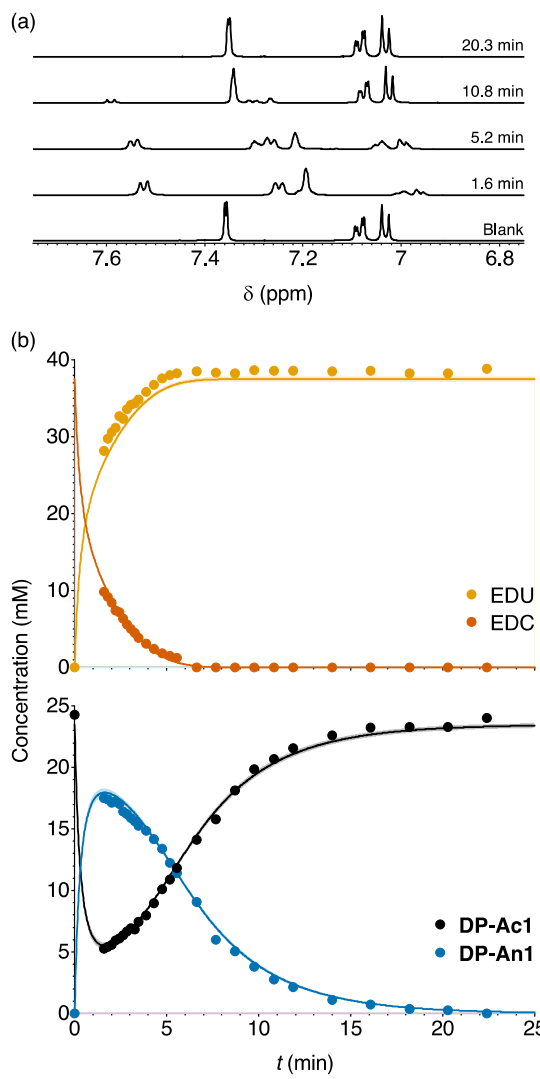
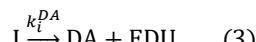
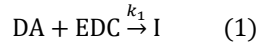


**Figure 2.** (a)  $^1\text{H}$  NMR spectroscopy of **DP-An1** formation upon the treatment of **DP-Ac1** (25 mM) with EDC (40 mM) in  $\text{D}_2\text{O}$ :acetone- $d_6$  at 276 K. (b) Concentration vs time for the **DP-Ac1/DP-An1** system ( $\text{D}_2\text{O}$ :acetone- $d_6$ , 7:3, 276 K) with the addition of 40 mM EDC to 25 mM **DP-Ac1**. Solid lines represent the fits to the kinetic model and the shaded areas represent 95% confidence intervals (in some cases the CIs are narrow enough to be difficult to distinguish from the line). Note that the fits were generated by fitting to all four experiments simultaneously.

In previous work, the addition of pyridine was necessary to avoid unproductive rearrangements of the *O*-acylisourea intermediate to the *N*-acylurea.<sup>27,28</sup> For the diphenic acids, no additives were necessary, as intramolecular ring closure is presumably fast enough to outcompete the rearrangement. The system can be “refueled” with additional EDC, with three cycles shown in the Supporting Information (Figure S2).

To better understand the mechanism, four kinetic runs were performed, varying the initial concentration of EDC ( $[\text{EDC}]_0$ ). The data was then fit to a simple kinetic model<sup>29-31</sup> that describes the broad features of the system but lacks some mechanistic details, such as the pH-dependence of the rate constants and EDC speciation.<sup>32</sup> Initial reaction of one carboxylic acid group in diphenic acid (DA) with EDC is expected to generate an *O*-acylisourea intermediate (I) (eq 1).

This intermediate can either react with the remaining acid group to form the anhydride (and EDU, eq 2), or it can undergo unproductive decomposition to reform the starting acid (and EDU, eq 3). The anhydride then hydrolyzes back to the starting acid (eq 4). A steady-state was assumed in I, which simplifies the parameters with  $\alpha = k_i^{\text{DA}}/k_i^{\text{An}}$ .



The differential equations describing this mechanism were fit numerically to the complete data set for **DP-Ac1** (see Supporting Information). A representative example of the fit is shown in Figure 2b. Uncertainties (95% confidence interval) for the regression were estimated by applying a non-parametric bootstrapping method,<sup>27</sup> and were reasonable (shaded in Figure 2b). The resulting apparent rate constants for the **DP-Ac1** system under these conditions are  $k_1 = (8.77^{+0.39}_{-0.37} \times 10^{-2}) \text{ mM}^{-1}\text{min}^{-1}$ ,  $k_2 = (2.576^{+0.069}_{-0.071} \times 10^{-1}) \text{ min}^{-1}$ , and  $\alpha = 1.13^{+0.08}_{-0.14} \times 10^{-1}$ . Confidence contour plots were generated to confirm the independence of the parameters (see Supporting Information).<sup>33</sup>

While these kinetic parameters fully describe the system, it can be helpful to translate them into terms that are more intuitive,<sup>27</sup> such as the peak anhydride concentration ( $[\text{An}]_{\text{max}}$ ), the acid recovery time ( $\tau_{99}$ , the time it takes for the **DP-Ac1** to return to 99% of its starting value), and the anhydride yield (the net quantity of anhydride produced relative to the amount of EDC added). For this mechanism, the yield is dependent on the partitioning of I between the anhydride (eq 2) and direct hydrolysis (eq 3), and is therefore a simple function of  $\alpha$  (yield =  $1/(1 + \alpha)$ ). The **DP-Ac1** system is very efficient, with a yield of  $90^{+2}_{-6}\%$ .

The peak anhydride concentration and the lifetime are both dependent on the starting concentrations of acid and carbodiimide but can be simulated from the parameters. The results of simulations of the reaction of **DP-Ac1** (25 mM) with variable amounts of starting EDC ( $[\text{EDC}]_0$ ) are shown in Figure 3. As expected,  $[\text{An}]_{\text{max}}$  increases rapidly with increasing  $[\text{EDC}]_0$ , approaching a limit near the starting acid concentration (Figure 3a). Because hydrolysis is relatively slow compared to activation, it takes relatively little EDC to push the system to high conversion. The recovery time  $\tau_{99}$  shows a sharp increase initially with increasing EDC, but then increases only slowly (Figure 3b).

We then turned to substituted derivatives **DP-Ac2** and **DP-Ac3** to determine the ability of this chemistry to act against steric resistance, which will affect its usefulness in functional systems. On treatment of both diacids with EDC, we again observe the formation of new species by  $^1\text{H}$  NMR spectroscopy. These were confirmed to be the expected anhydrides **DP-An2** and **DP-An3** by comparison with independently synthesized samples (see Supporting Information). Concentration vs time data is shown in Figure 4

(and S16/S17). It is clear that the chemistry works effectively: the corresponding anhydrides form and decay as expected. The overall time scale of the reactions are longer, particularly for **DP-Ac3**. Curiously, the data obtained for **DP-Ac2** and **DP-Ac3** indicate that the hydration of EDC seems to go through two phases: faster very early on but then slowing significantly. This is possibly due to the changing pH during the reactions as the starting acids are consumed, although it is not immediately obvious why the effect is more pronounced for these systems compared to **DP-Ac1**.

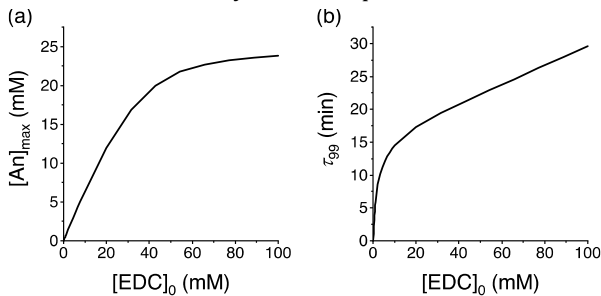


**Figure 3.** Simulated behavior of the **DP-Ac1** (25 mM) system with variable addition of EDC. (a) Peak anhydride concentration  $[An]_{\max}$  vs  $[EDC]_0$ . (b) Time to recover 99% of the starting acid  $\tau_{99}$  vs  $[EDC]_0$ .

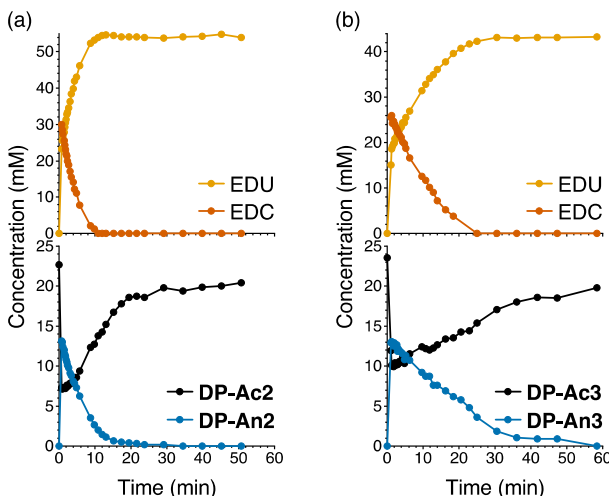


**Figure 4.** Representative examples of transient anhydride formation from substituted diphenic acids ( $D_2O$ :acetone- $d_6$ , 7:3, 276 K). (a) **DP-Ac2** with the addition of 2 equiv EDC. (b) **DP-Ac3** with the addition of 2 equiv of EDC. Note that the initial concentration of EDC cannot be measured in these systems as its consumption begins immediately upon mixing outside of the NMR spectrometer.

Unfortunately, the NMR data for substituted derivatives failed to yield good fits to the simple mechanism described above. Even after treating with relatively large amounts of EDC, the maximum conversion peaks at about 50%, in contrast to the unsubstituted system (compare Figures 4 and 2b). There is evidence that the formation of byproducts, likely intermolecular anhydrides, becomes significant with higher concentrations of EDC: some broad unassigned peaks appear and disappear during the  $^1H$  NMR experiments in the substituted systems (Figure S9), and it takes a longer time to fully recover the starting acids **DP-Ac2** and **DP-Ac3**. We believe that these byproducts are the result of

intermolecular oligomerization, as steric hindrance in **DP-Ac2** and **DP-Ac3** disfavors cyclization. Unfortunately, these species could not be characterized or quantified. We are currently working toward experimental conditions that will yield cleaner data for these systems. Nevertheless, it is noteworthy that substantial amounts of anhydride are formed even for these more-demanding diacids, which bodes well for integrating these units within more-complex systems.

Our findings demonstrate that intramolecular anhydrides can be formed from substituted diphenic acids using EDC as a chemical fuel, leading to a transient change in the geometry of the molecule. This provides a simple platform to mimic the conformational changes observed in biological systems. More work on optimizing reaction conditions to better quantify the behavior of substituted diphenic acids, and the study of other substituted derivatives, is underway.

## ASSOCIATED CONTENT

### Supporting Information

The Supporting Information is available free of charge on the ACS Publications website.

Experimental procedures, IR spectra, computational chemistry details, NMR spectra, details on kinetics analysis (PDF)

Computational geometries (TXT)

Concentration vs time data (TXT)

Python program used to analyze kinetics (ZIP)

## AUTHOR INFORMATION

### Corresponding Author

\* E-mail: scott.hartley@miamioh.edu

### Author Contributions

The manuscript was written through contributions of all authors. All authors have given approval to the final version of the manuscript.

## ACKNOWLEDGMENT

This work was supported by the U.S. Department of Energy, Office of Science, Basic Energy Sciences, under Award # DE-SC0018645. The purchase of the 400 MHz NMR spectrometer was supported by the National Science Foundation (CHE-1919850).

## REFERENCES

- (1) Mattia, E.; Otto, S. *Nat. Nanotechnol.* **2015**, *10*, 111–119.
- (2) Whitesides, G. M.; Grzybowski, B. *Science* **2002**, *295*, 2418–2421.
- (3) Astumian, R. D. *Proc. Natl. Acad. Sci. U.S.A.* **2018**, *115*, 9405–9413.
- (4) Astumian, R. D. *Chem. Commun.* **2018**, *54*, 427–444.
- (5) van Rossum, S. A. P.; Tena-Solsona, M.; van Esch, J. H.; Eelkema, R.; Boekhoven, J. *Chem. Soc. Rev.* **2017**, *46*, 5519–5535.
- (6) Vale, R. D.; Milligan, R. A. *Science* **2000**, *288*, 88–95.
- (7) Wang, H.; Oster, G. *Nature* **1998**, *396*, 279–282.
- (8) Higgins, C. F.; Linton, K. J. *Nat. Struct. Mol. Biol.* **2004**, *11*, 918–926.
- (9) Roberts, A. J.; Kon, T.; Knight, P. J.; Sutoh, K.; Burgess, S. A. *Nat. Rev. Mol. Cell Biol.* **2013**, *14*, 713–726.
- (10) Cochran, J. *Biophys. Rev.* **2015**, *7*, 269–299.

(11) Boekhoven, J.; Hendriksen, W. E.; Koper, G. J. M.; Eelkema, R.; van Esch, J. H. *Science* **2015**, *349*, 1075–1079.

(12) Wilson, M. R.; Solà, J.; Carbone, A.; Goldup, S. M.; Lebrasseur, N.; Leigh, D. A. *Nature* **2016**, *534*, 235–240.

(13) Rieß, B.; Grötsch, R. K.; Boekhoven, J. *Chem* **2020**, *6*, 552–578.

(14) Tena-Solsona, M.; Rieß, B.; Grötsch, R. K.; Löhrer, F. C.; Wanzke, C.; Käsdorf, B.; Bausch, A. R.; Müller-Buschbaum, P.; Lieleg, O.; Boekhoven, J. *Nat. Commun.* **2017**, *8*, 15895.

(15) Grötsch, R. K.; Wanzke, C.; Speckbacher, M.; Angi, A.; Rieger, B.; Boekhoven, J. *J. Am. Chem. Soc.* **2019**, *141*, 9872–9878.

(16) Hossain, M. M.; Atkinson, J. L.; Hartley, C. S. *Angew. Chem., Int. Ed.* **2020**, *59*, 13807–13813.

(17) Zhang, B.; Jayalath, I. M.; Ke, J.; Sparks, J. L.; Hartley, C. S.; Konkolewicz, D. *Chem. Commun.* **2019**, *55*, 2086–2089.

(18) Bal, S.; Das, K.; Ahmed, S.; Das, D. *Angew. Chem., Int. Ed.* **2019**, *58*, 244–247.

(19) Bal, S.; Ghosh, C.; Ghosh, T.; Vijayaraghavan, R. K.; Das, D. *Angew. Chem., Int. Ed.* **2020**, *59*, 13506–13510.

(20) Cheng, M.; Qian, C.; Ding, Y.; Chen, Y.; Xiao, T.; Lu, X.; Jiang, J.; Wang, L. *ACS Materials Lett.* **2020**, *2*, 425–429.

(21) Panja, S.; Dietrich, B.; Adams, D. J. *ChemSystemsChem* **2019**, *2*, e1900038.

(22) Kariyawasam, L. S.; Hartley, C. S. *J. Am. Chem. Soc.* **2017**, *139*, 11949–11955.

(23) A preprint of this manuscript was deposited in ChemRxiv, DOI: 10.26434/chemrxiv.12808091.

(24) Jalani, K.; Dhiman, S.; Jain, A.; George, S. J. *Chem. Sci.* **2017**, *8*, 6030–6036.

(25) Wang, D. H.; Cheng, S. Z. D.; Harris, F. W. *Polymer* **2008**, *49*, 3020–3028.

(26) Kitagawa, T.; Kuroda, H.; Sasaki, H. *Chem. Pharm. Bull.* **1987**, *35*, 1262–1265.

(27) Kariyawasam, L. S.; Kron, J. C.; Jiang, R.; Sommer, A. J.; Hartley, C. S. *J. Org. Chem.* **2020**, *85*, 682–690.

(28) DeTar, D. F.; Silverstein, R. J. *Am. Chem. Soc.* **1966**, *88*, 1013–1019.

(29) Mironova, D. F.; Dvorko, G. F. *Ukr. Khim. Zh. (Russ. Ed.)* **1967**, *33*, 602–614.

(30) Ibrahim, I. T.; Williams, A. J. *Chem. Soc., Perkin Trans. 2* **1982**, 1459–1466.

(31) Berliner, E.; Altschul, L. H. *J. Am. Chem. Soc.* **1952**, *74*, 4110–4113.

(32) Ibrahim, I. T.; Williams, A. J. *Am. Chem. Soc.* **1978**, *100*, 7420–7421.

(33) Johnson, K. A.; Simpson, Z. B.; Blom, T. *Anal. Biochem.* **2009**, *387*, 30–41.